Electrochemical Performance of Polymer and Potassium Salt Electrolyte

THESIS

Presented in Partial Fulfillment of the Requirements for Graduation with Honors Research Distinction in Chemistry at The Ohio State University

By

Justin T. Dilenschneider

B.S. Program in Chemical & Biomolecular Engineering

The Ohio State University

Department of Chemistry and Biochemistry

2018

Thesis Committee

Dr. Yiying Wu, Advisor

Dr. Nicholas Brunelli, Co-Advisor

Dr. Lisa Hall

Abstract

Current batteries require further research to fulfil the stability, cost, and energy requirements of modern technology. Potassium-oxygen batteries show promise in their large specific energy and high round-trip efficiency; however, further research is required develop this technology. Using a polymer-in-salt electrolyte instead of an organic based electrolyte could improve the cycle life of the battery while retaining its efficiency and performance. As of yet, little research has been conducted to determine the performance of these polymer-in-salt electrolytes in potassium-oxygen batteries. The goal of this study was to investigate the performance of the KMPSA salt and PEO (polyethylene oxide) polymer mixture in a potassium-oxygen battery. Coarse-grained molecular simulations within LAMMPS were conducted with different weight ratios of KMPSA. These simulations provided insight into how the electrolyte behaved. In addition, theoretical conductivity was calculated once the system achieved equilibrium. KMPSA was synthesized, characterized, and mixed with prepared PEO ($M_n = 4 \times 10^3$) to produce a viscous electrolyte. Attempts to test this electrolyte in a potassium-oxygen battery produced inconclusive results.

Acknowledgments

I would like to thank Dr. Wu for providing his time, lab, and equipment to foster my growth as a researcher.

I would like to thank Dr. Wu's graduate students for teaching me and helping me in lab. I greatly appreciate all of the time they sacrificed to assist me and answer my questions. Specifically, I would like to thank William McCulloch (Billy) for his mentorship.

Additionally, I would like to thank Dr. Brunelli for being a steady source of advice as my co-advisor. I would also like to thank Dr. Hall for teaching me about simulations and molecular modeling. A special thanks to Jopam Merichi as well.

Finally, I would like to thank The Ohio State University for providing the opportunity to conduct meaningful research as an undergraduate.

Table of Contents

List of Tables

List of Figures

Introduction

Battery Technology

With the growing energy storage needs of technology, batteries with larger energy density and stability are required to keep pace. Electric vehicles, for example, require compact electricity storage to compete with gasoline. Current rechargeable battery technology boasts an energy density up to 1000 Wh/kg depending on the type [1] whereas gasoline has a specific energy around 12,000 Wh/kg [2]. Figure 1 summarizes this comparison.

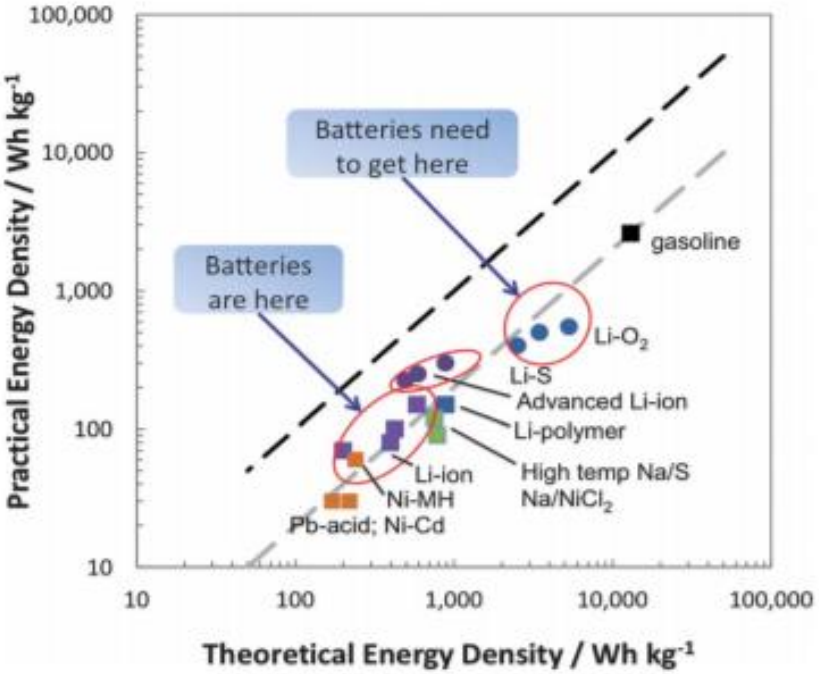

Figure 1: Energy Densities of Battery Technology [1]

Improving battery technology also helps a variety of other modern technological applications. A larger energy density would equate to longer battery life for phones of equal size or compact storage for a renewable energy grid. Equally important is the cycle life of a battery, or how many times a battery can be charged/discharged before deteriorating significantly. Longer lasting batteries are greatly needed for renewable energy applications where batteries would be charged and discharged many times due to the intermittent power supply of renewable energy sources. To help make electric vehicles and renewable energy more feasible and attractive, both the cycle life and the energy density of current batteries need to be improved.

Researchers are investigating many different avenues to improve battery technology. An emerging battery technology, the metal-oxygen battery, is a possible route that could significantly increase the energy density of batteries. Current research conducted on Li-O_2 batteries has found an energy density of up to 3505 Wh/kg [3] which is superior to that of other established battery technology. However, a lot of complications exist with Li-O_2 battery technology such as high overpotentials, problematic side reactions, and low round-trip efficiencies around 60%. Specifically, the charging overpotential is significantly higher than the discharge overpotential due to asymmetric reactions in the battery [3].

Potassium-oxygen batteries are able to form a thermodynamically stable superoxide species (KO_2) during discharge that reduces the highly asymmetric overpotentials seen in Li-O_2 batteries [3]. So far, potassium-oxygen batteries boast lower

overpotentials allowing it to operate around a 95% round-trip efficiency with a theoretical energy density of 935 Wh/kg [3].

Electrolytes in a Battery

Even with more stable formation of the superoxide species, potassium-oxygen batteries still need a variety of improvements before they can compete with the current technology. One major concern for any battery is its electrolyte. Electrolytes need to be able to transfer ions between the anode and cathode of the battery while remaining electrochemically stable at both interfaces. Liquid electrolytes have high ionic conductivities (10^{-3} to 10^{-2} S/cm), but typically use volatile solvents that bring a variety of safety concerns including leakage and high flammability [11]. Additionally, liquid electrolytes made with organic solvents can cause decomposition reactions [10]. On the other hand, solid electrolytes made with polymers boast versatile mechanical properties, but poor surface contact with the electrodes and low ionic conductivity (10^{-8} to 10^{-5} S/cm) [11]. Ideally, an electrolyte would have a reasonable ionic conductivity without any need for unsafe organic electrolytes.

In general, ionic conductivity is greater in disordered systems which explains the low conductivity of polymers and high conductivity of binary liquid electrolytes [5]. Polymers can be combined with other materials to increase their conductivity while still retaining some of the beneficial mechanical properties. Electrolytes that combine polymers and salts to create a mixture are known as salt-in-polymer or polymer-in-salt electrolytes depending on which weight percent dominates the mixture.

This study focuses on a particular polymer-in-salt electrolyte, PEO-in-KMPSA, and its application in a potassium-air battery. The PEO-in-KMPSA mixture was chosen due to its low glass transition temperature and amorphous state at room temperature, shown in Figure 2.

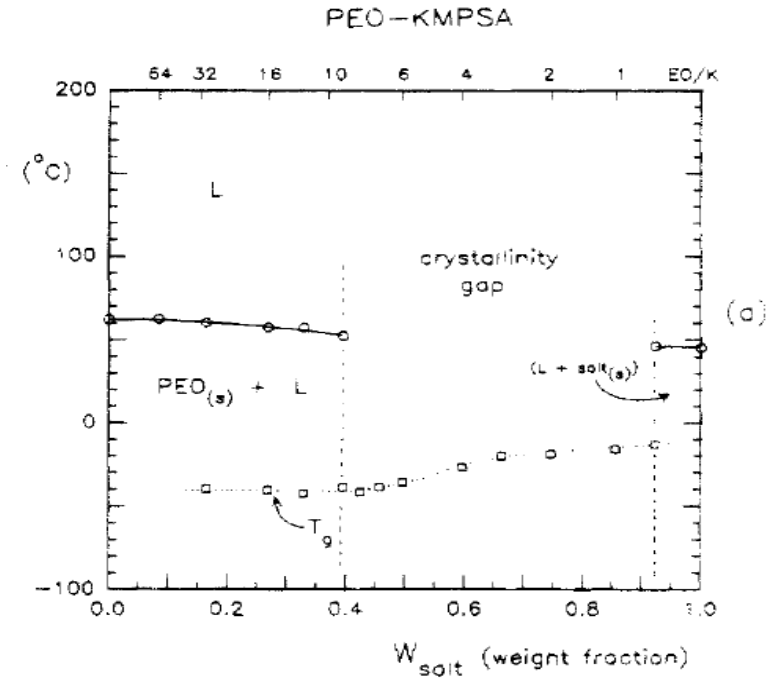

Figure 2: Phase Diagram for PEO-KMPSA Mixture [6]

To study the performance of this polymer-in-salt electrolyte, the mixture was first properly synthesized and characterized. Secondly, coarse-grained molecular dynamic simulations were conducted to calculate a theoretical conductivity. Finally, a potassium-oxygen battery was constructed and analyzed with the PEO-in-KMPSA electrolyte.

Methods

Synthesis of PEO-KMSPA Mixture

N-(3-Methoxypropyl)trifluoromethanesulfonamide, $CF_3SO_2NH(CH_2)_3$-OCH_3, (HMPSA) was synthesized by reacting 3-methoxypropylamine (Sigma-Aldrich, 99%) and trifluoromethanesulfonic anhydride (TCI America) in the presence of triethylamine (Sigma-Aldrich, >99%) shown in Figure 3. The anhydride was kept under dry conditions and added under cooling (-30 ºC) to the reactants under an inert atmosphere in dichloromethane (Acros Organics, Extra Dry). The reaction mixture was allowed to react at room temperature for 3 hours. The solvent was evaporated using a rotary evaporator, and the resulting residue was mixed with 4M NaOH. Organic byproducts were extracted with dichloromethane, while the resulting aqueous phase was neutralized with HCl. The organic phase of this solution was extracted with dichloromethane and dried with magnesium sulfate. Finally, the solution was filtered and the solvent was evaporated under vacuum.

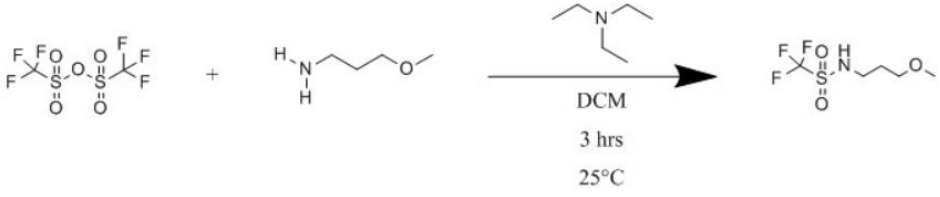

Figure 3: HMPSA Reaction Scheme

KMPSA was prepared by reacting HMPSA with excess K_2CO_3 (Alfa Aesar, 99%, anhydrous) in acetonitrile (Sigma-Aldrich, 99.8%, anhydrous), shown in Figure 4, under

an inert atmosphere for 24-96 hours with longer times achieving better yields. The excess K_2CO_3 was removed via filtration and the solvent was evaporated using a rotary evaporator. The resulting salt was further dried for 24 hrs at 70 ºC under vacuum. The KMPSA took a couple days to fully crystalize once cooled and was stored under an inert atmosphere.

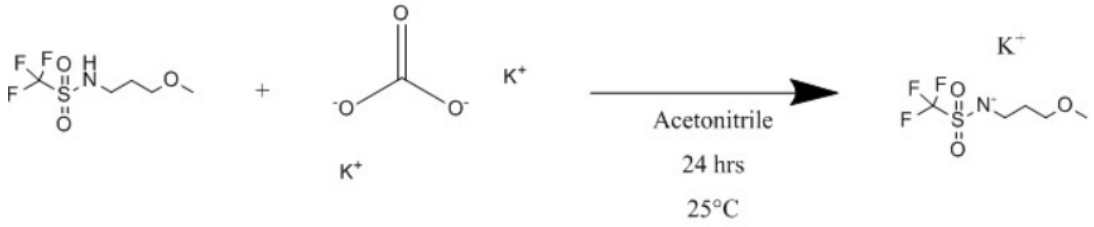

Figure 4: KMPSA Reaction Scheme

Poly(ethylene oxide) (Sigma, M_n = 4000), PEO, was purified by dissolving it in a 5 wt% tetrahydrofuran (Acros Organics) solution under heating (~45 ºC), then slowly adding this solution to double the volume of hexanes (Sigma-Aldrich). The solution was allowed to rest for 1 hr and then filtered and dried under vacuum for 48 h to produce a fine, white powder. This powder was stored under an inert atmosphere.

5 wt% methanol (Acros Organics, 99.9%, Extra Dry, AcroSeal) solutions of both PEO and KMSPA were mixed together under an inert atmosphere for 1 hr. After solvent evaporation with a rotary evaporator, the mixture was dried under vacuum at 70 ºC for 12-24 hr.

Battery Assembly

Potassium-oxygen batteries were assembled under an inert atmosphere, and then purged with oxygen and sealed. Cells were constructed using solid potassium metal as the

anode, Celgard film (25 µmT x 85 mm W) and glass microfibre filter (Whatman, GF/A) as the separator material, porous carbon (Fuel Cell Earth, P50) as the cathode, and stainless-steel mesh (Alfa Aesar, Type 316) as the cathode current collector. Prior to assembly, the separators were soaked in electrolyte solution for 12-24 hrs.

Battery testing was done using an MTI Battery Analyzing System. A small current of 0.02 mA was used for testing along with charging and discharging voltage limits of 3.2 V and 1.8 V respectively.

Molecular Dynamics Simulations

The KMPSA salt was modeled with a free-floating K+ cation (Type 3) and two bonded beads: one anion (Type 2) and one PEO monomer (Type 1). The PEO was modeled with 60 bonded beads of Type 1 monomers. Initial positions were determined using a random walks python script and the simulations were carried out using LAMMPS software through the Ohio Supercomputer Center (OSC). Reduced Lennard-Jones units were used where $\sigma = 0.461$ nm, which is the S-S distance between two $MPSA^-$ anions (from LiMPSA data) [7]. The finite extensible nonlinear elastic (FENE) potential was used to describe bond interactions (Figure 5).

$$E = -0.5KR_0^2 \ln\left[1 - \left(\frac{r}{R_0}\right)^2\right] + 4\epsilon\left[\left(\frac{\sigma}{r}\right)^{12} - \left(\frac{\sigma}{r}\right)^{6}\right] + \epsilon$$

Figure 5: FENE Potential Equation

Constants $K = 30$, $R_0 = 1.5$, $\varepsilon = 1.0$, and $\sigma = 1.0$ were used to keep atoms bonded closely together without overlapping.

Pairwise interactions were initially determined using a soft potential shown in Figure 6 to ease the beads off one another.

$$E = A\left[1 + \cos\left(\frac{\pi r}{r_c}\right)\right] \qquad r < r_c$$

Figure 6: Soft Potential in LAMMPS [8]

Where A was a pre-factor varied that was varied from 0.0 to 50.0 in 1000 timesteps. In addition, r_c (cutoff) was specified as $2^{1/6}$. On top of this, an NVE ensemble with a temperature velocity rescaling from 0.0 to 1.0 was used for 5000 timesteps (1 timestep = 0.0115 tau).

After the initial push off, the pairwise interactions between all beads were dictated by a cut Leonard-Jones potential (Figure 7) while the ionic interactions had an additional long-range Coulomb potential (Figure 8). A custom potential from Dr. Hall based on $1/r^4$ that accounted for the solvation of ions into the PEO was applied between monomers and ions [14].

$$E = 4\epsilon\left[\left(\frac{\sigma}{r}\right)^{12} - \left(\frac{\sigma}{r}\right)^{6}\right] \qquad r < r_c$$

Figure 7: Lennard-Jones Potential [8]

$$E = \frac{Cq_iq_j}{\epsilon r} \qquad r < r_c$$

Figure 8: Coulomb Potential [8]

An additional particle-particle particle-mesh solver was used with an absolute charge value cutoff of 1.0e-4. The constants applied to each potential were chosen based on the KMPSA molecule and a temperature of 300 K as shown in Table 1.

Parameters	σ	Ɛ	Cutoff(σ)
LJ	1	1	2.5
Born Solvation	1	3.18	5
Coulomb	N/A	N/A	6.2

Table 1: Potential Constants

A dielectric constant of 0.062 was used to represent charged interactions not captured by the coarse-grained simulation. An NPT ensemble with a Nose-Hoover thermostat/barostat was used to keep pressure at 0.0 and temperature at 1.0. Once the volume was constant, the simulation was restarted with an NVT ensemble using the same thermostat as before. Simulations were typically run around 10 million timesteps to reach equilibration.

To change the composition of the polymer-in-salt mixture, a formula was derived to calculate the number of polymer and salt molecules depending on select variables (Figure 9).

$$N_s = \frac{B_T X_s MW_p}{X_p MW_s A_p + X_s MW_p A_s} \quad N_p = \frac{B_T - A_s N_s}{A_p}$$

Figure 9: Number of Salt/Polymer Molecule Formulae

Where B_T = Total Number of Beads, N = Number of Molecules, MW = Molecular Weight, X = Mass Fraction, A = Number of Beads/Molecule and subscripts s = salt, p = polymer. Each simulation preserved ~10,000 total beads and assumed a short polymer length of 60 beads per molecule to avoid entanglement of the polymer. Each salt molecule contained 3 beads as well.

Results and Discussion

Protocol Development

The synthesis of KMPSA required many attempts to obtain a pure, clear sample. Many impurities can be introduced throughout the synthesis process that can cause the desired clear substance to be tinted. Small amounts of impurities can change the behavior of the KMPSA salt, especially as used in an electrolyte. Therefore, a pure, limpid sample is needed to properly test the material. This section will detail steps that were problematic in the synthesis not addressed in the methods section and discuss how to overcome these issues. Pure samples of HMPSA were characterized visually and by using Nuclear Magnetic Resonance (NMR) shown in Figure 10.

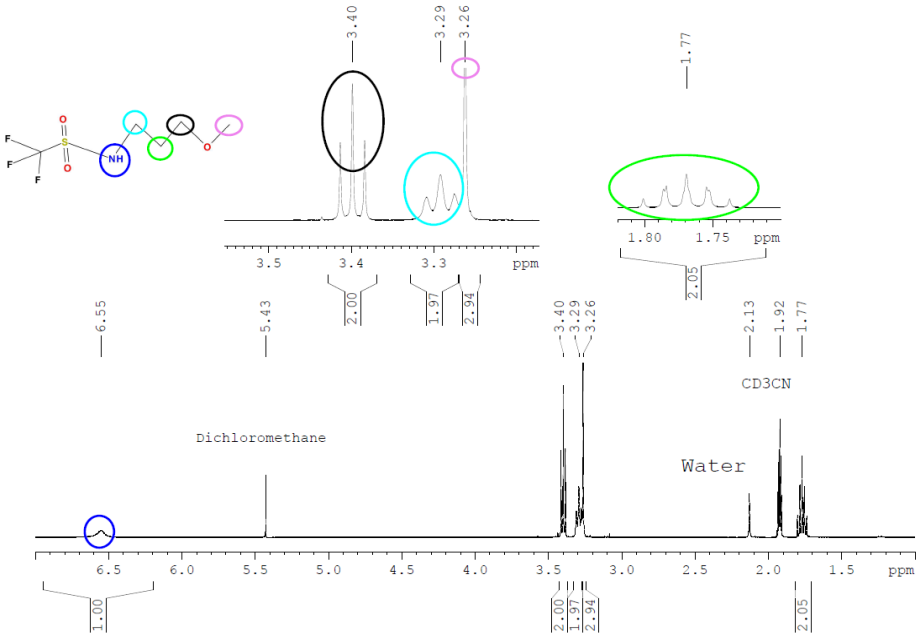

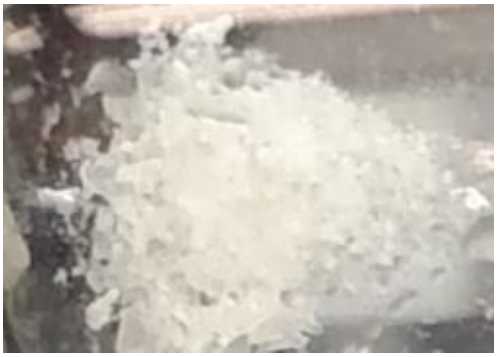

Figure 10: NMR of HMPSA (Left) and Picture of KMPSA (Right)

First, a distillation step added at the end of the extraction step for HMPSA helped remove color impurities. These impurities were likely species that were not extracted out during the extraction process. Secondly, the drying steps caused many issues during the synthesis. The high temperatures required by the protocol can degrade many materials including sharpie labels, stoppers, syringes with plastic, and lids with septa all of which can introduce impurities. These impurities were made evident by a tinted liquid after drying. Removing these materials as well as reducing the heating temperatures helped eliminate the unwanted color. Finally, some stoppers would introduce impurities by simply contacting the liquid and depositing surface contaminants.

Simulation Results

A 50-50 wt% KMPSA-PEO system was simulated along with a 70-30 wt% KMPSA-PEO system. Pair correlation functions and ionic conductivities were calculated for all systems. Images and pair correlation functions were created using Visual Molecular Dynamics (VMD) software from the University of Illinois at Urbana-Champaign [9]. Pair correlation functions were calculated by averaging over ~100 snapshots after equilibration of the system. The ionic conductivity was averaged over 30 non-overlapping blocks with 20 snapshots each using a python script and Figure 11 that tracks the ions' center of mass movement.

$$\sigma = \lim_{t\to\infty} \frac{e^2}{6tVk_BT} \sum_{i,j}^{N} z_i z_j \left\langle [r_i(t) - r_i(0)][r_j(t) - r_j(0)] \right\rangle \qquad \langle \{[\sum_+ \boldsymbol{r}(t) - \sum_- \boldsymbol{r}(t)] - [\sum_+ \boldsymbol{r}(0) - \sum_- \boldsymbol{r}(0)]\}^2 \rangle$$

Figure 11: Ionic Conductivity Equation (left) with simplified sum term (right) [13]

Figure 12 and Figure 13 show the visualization of both systems at three different timesteps with red: $MPSA^-$ anion, black: K^+ cation, and pink: PEO monomer. The box volume is fully occupied after the initial placement and the ordering of beads has no visual pattern. In addition, the higher KMPSA wt% system shows a larger number of ions in the system as expected. However, the positions of the beads in the second system do not change as much as the first system.

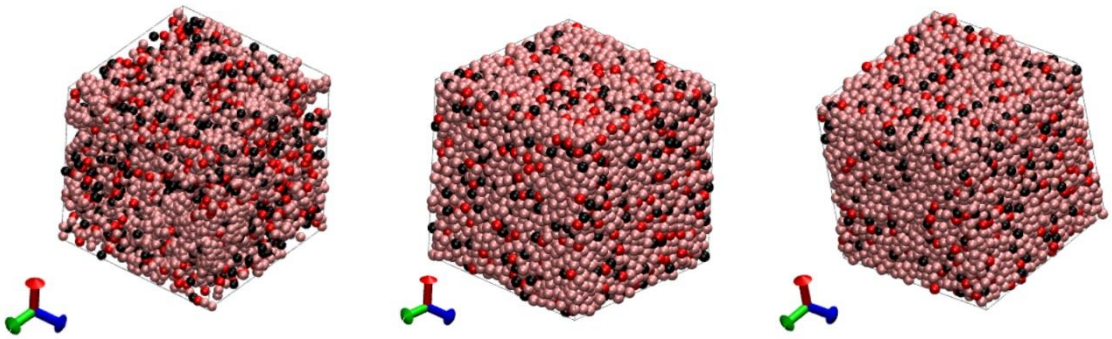

Figure 12: VMD Images of 50 wt% KMPSA: Initial, 6 million timesteps, 11 million timesteps

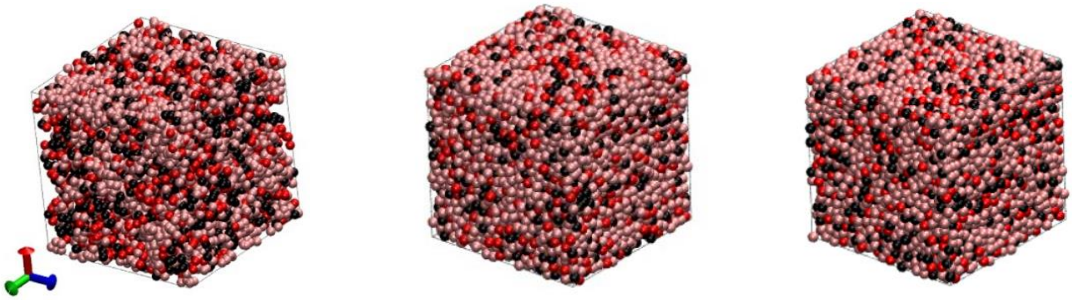

Figure 13: VMD Images of 70 wt% KMPSA: Initial, 2.5 million timesteps, 5 million timesteps

Due to the lack of holes and disorder in the system, these simulations visually appear to match the description of an amorphous liquid. To understand the ordering of the system better, the pair correlation functions were compared in Figure 14 and Figure 15 on the next page. Each system showed similar tends. The oppositely charged

interactions (2-3) had a sharp, tall peak due to the strength of the ionic forces. The PEO's interaction with itself (1-1) had a smaller peak at 1σ due to the bonds formed between monomers 1σ away. Finally, the similarly charged ion interactions (2-2, 3-3) had peaks at a farther distance away due to their repelling forces.

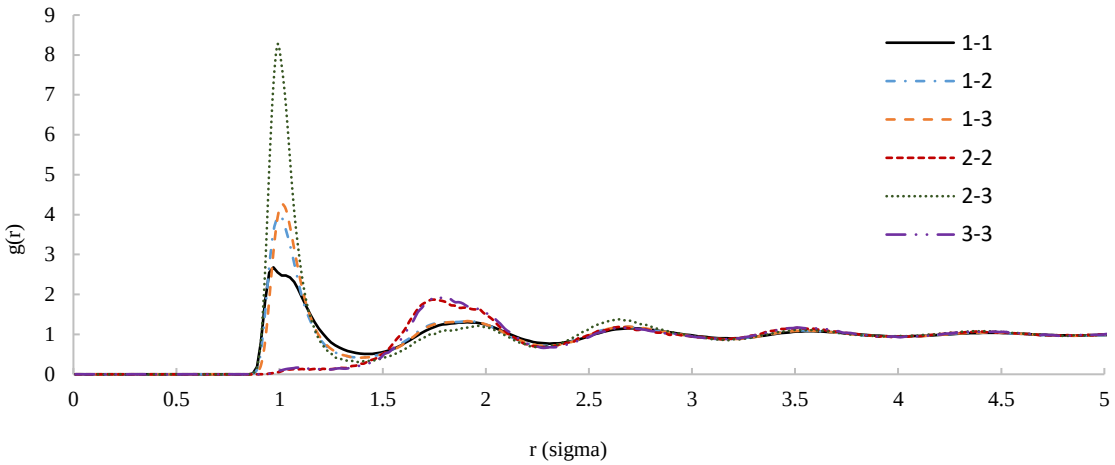

Figure 14: Pair Correlation Function for 50 wt% KMPSA. 1 = PEO monomer, 2 = $MPSA^-$ Anion, 3 = K^+ Cation

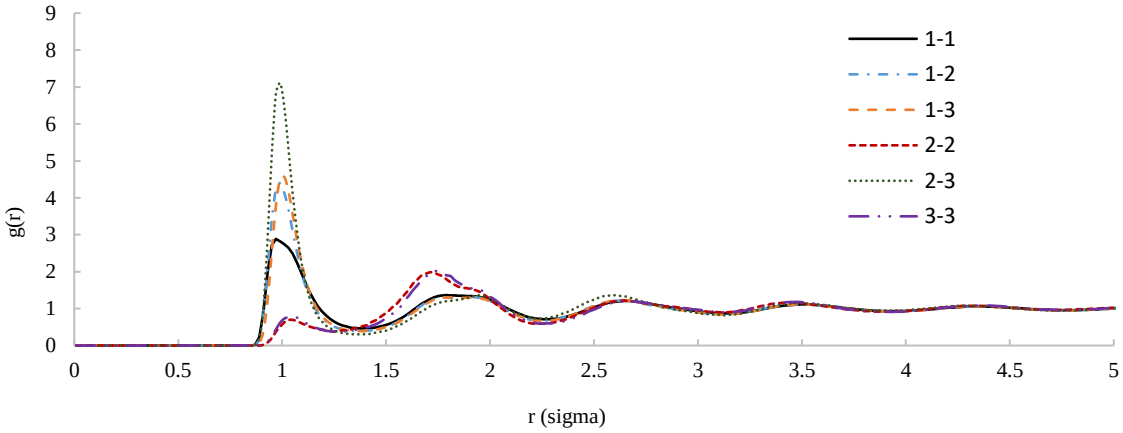

Figure 15: Pair Correlation Function for 70 wt% KMPSA. 1 = PEO monomer, 2 = $MPSA^-$ Anion, 3 = K^+ Cation

Using the positional data of the beads, the summation term in Figure 11 was calculated for both systems shown in Figure 16 and Figure 17. The 50 wt% mixture had much higher ionic movement and higher slope than the 70 wt% mixture.

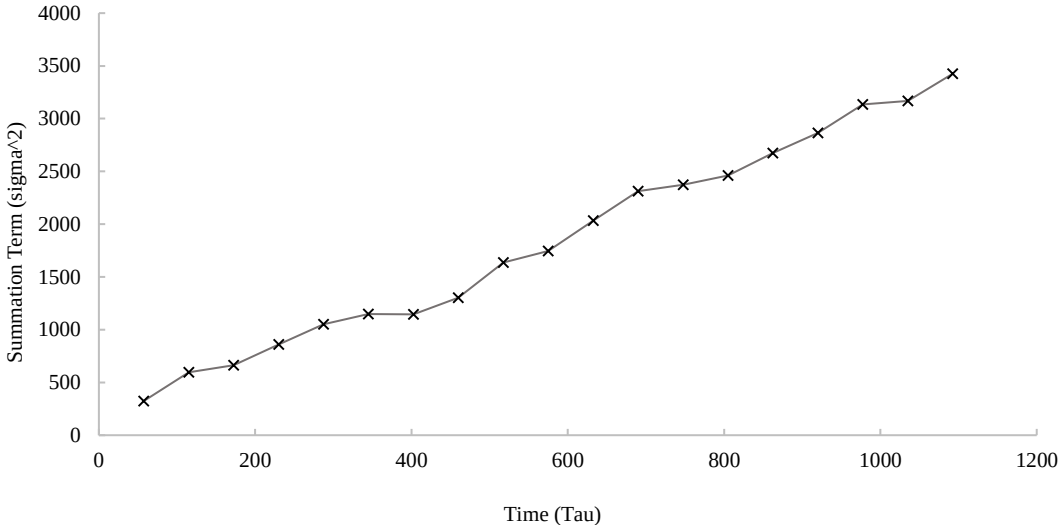

Figure 16: Conductivity Summation Term for 50 wt% KMPSA

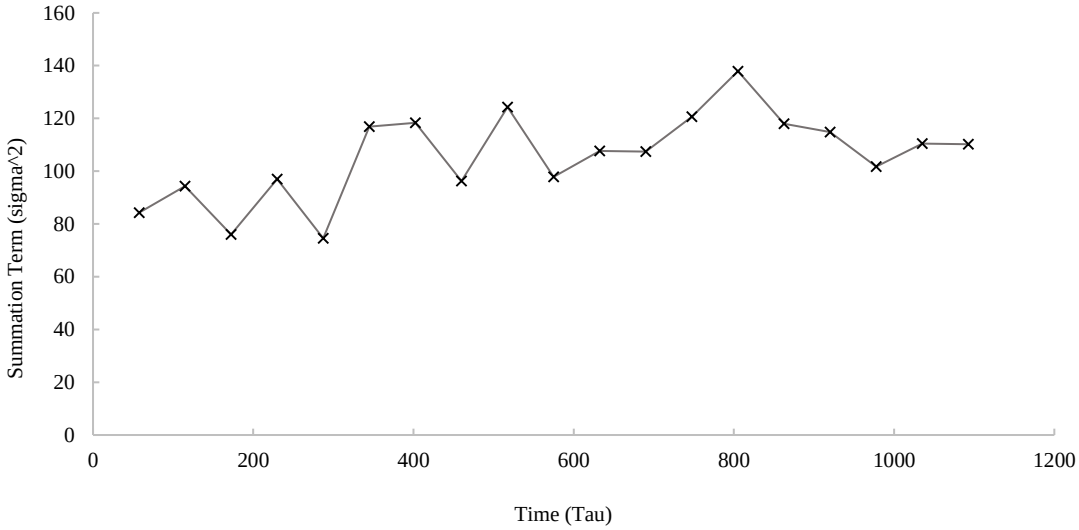

Figure 17: Conductivity Summation Term for 70 wt% KMPSA

The ionic conductivity of each system was calculated by mapping the reduced units to real units with $\sigma = 0.461$ nm and $T = 300$ K. These conductivities were compared to the experimental results found by Prud'homme et al. in Table 2.

wt% KMPSA	Calculated Conductivity (S/cm)	Literature Conductivity (S/cm)	Percent Difference (%)
50	1.09E-05	3.58E-05	106.6
70	1.08E-07	6.40E-06	193.4

Table 2: Conductivity comparison to literature values @ 318K [6]

As the KMPSA composition increases in the amorphous phase, the conductivity appears to decrease for the simulation results. Compared to literature, the 50 wt% KMPSA matched well considering the simulation was run at a lower temperature. However, the 70 wt% KMSPA had an almost 200% difference between the values. In addition, the low amount of ionic movement in the 70 wt% KMPSA mixture does not resemble a liquid amorphous system. Regardless, the decreasing trend for both simulation and literature matched.

Battery Testing

Four batteries were assembled and tested all producing similar results summarized by Figure 18 on the next page. Each battery was discharged first and tested for at least 10 cycles with one minute in between each charge and discharge.

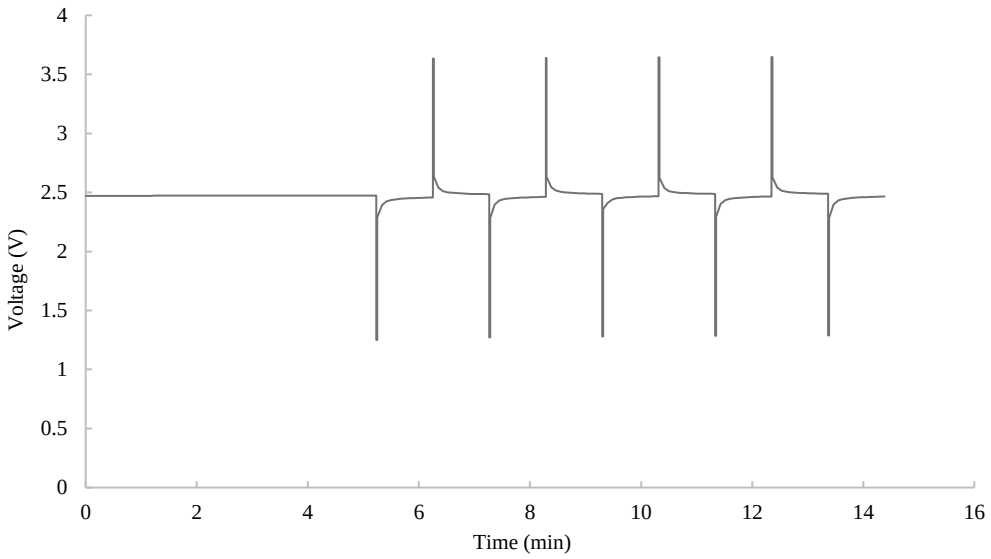

Figure 18: K-O_2 Battery 50 wt% PEO in KMPSA

The theoretical open-circuit voltage (OCV) for potassium-oxygen batteries is 2.48 V [3]. While the battery reached a suitable OCV, both discharge and charge curves had extremely high overpotentials resulting in a rapid spike or drop in voltage when applying or drawing current. Since a small amount of current was used in testing (0.02 mA), the high overpotential must be caused by a high resistance in the battery. Based on visual inspection, this resistance was likely caused by inadequate wetting of the separator materials by the viscous electrolyte in the battery.

Conclusions

First, the synthesis of the KMPSA salt and polymer mixture required additional steps to obtain a pure product. Many of the tasks to synthesize KMPSA needed to be done with great care to avoid introducing contaminants. The addition of a distillation step after synthesizing the HMPSA was also beneficial to achieving a pure result.

Second, the molecular simulations conducted were proven to match the expected real system in terms of its structure. In addition, the conductivities calculated from the simulations found that increasing KMPSA composition decreased ionic conductivity, which matched the trend found in literature. However, the large disparity between simulation and experimental conductivities for the mixtures with more KMSPA suggests that as more ions are introduced, the simulation might not be adequately representing the true system.

Lastly, the battery tests produced inconclusive results about any electrochemical performance of the polymer-in-salt electrolyte. The results did indicate, however, that the resistance in the battery was too high to conduct any meaningful tests. The cause of this issue was likely inadequate wetting of the separators.

Future Work

Many aspects of this study are limited in scope and could be expanded upon in the future. Ultimately, the high resistance in the potassium-oxygen battery inhibited any electrochemical performance data to be collected. Improving the separator materials or investigating a better wetting process (such as heating prior or during the wetting process) for the electrolyte would be the next step in advancing this research. Alternatively, this electrolyte system could be investigated as a possible gel-polymer electrolyte (GPE) without a separator [12]. Battery testing would ideally be done with different compositions of the polymer-in-salt, and possibly with different salts or polymers. Additionally, experimental conductivity tests could be performed to compare directly with the simulations.

In terms of modeling, more simulations at different compositions in the amorphous region would help clarify trends within the system. Also, other types of calculations could be performed on the simulation data to determine other properties such as viscosity. Simulations at different temperatures, specifically 318 K to help compare to Prud'homme at al., would help determine how the system behaves.

References

[1] Thackeray, M. M., Wolverton, C., & Isaacs, E. D. (2012). Electrical energy storage for transportation-approaching the limits of, and going beyond, lithium-ion batteries. *Energy & Environmental Science*, *5*(7), 7854–7863. https://doi.org/10.1039/C2EE21892E

[2] "Chapter 2." Energy: Production, Conversion, Storage, Conservation, and Coupling, by Springer Verlag, Springer Verlag, 2012, www.springer.com/cda/content/document/cda_downloaddocument/9781447123712-c2.pdf?SGWID=0-0-45-1293540-p174262962.

[3] Ren, X., & Wu, Y. (2013). A Low-Overpotential Potassium–Oxygen Battery Based on Potassium Superoxide. *Journal of the American Chemical Society*, *135*(8), 2923–2926. https://doi.org/10.1021/ja312059q

[4] Zhang, X., Wang, X.-G., Xie, Z., & Zhou, Z. (2016). Recent progress in rechargeable alkali metal–air batteries. Green Energy & Environment, 1(1), 4–17. https://doi.org/10.1016/j.gee.2016.04.004

[5] Polymer Electrolytes : Fundamentals and Applications, edited by César Sequeira, and Diogo Santos, Elsevier Science & Technology, 2010. ProQuest Ebook Central, https://ebookcentral-proquest-com.proxy.lib.ohio-state.edu/lib/ohiostate-ebooks/detail.action?docID=1585246.

[6] Lascaud, S., Perrier, M., Vallee, A., Besner, S., Prud'homme, J., & Armand, M. (1994). Phase Diagrams and Conductivity Behavior of Poly(ethylene oxide)-Molten Salt Rubbery Electrolytes. *Macromolecules*, *27*(25), 7469–7477. https://doi.org/10.1021/ma00103a034

[7] Dillon, R. E. A., Stern, C. L., & Shriver, D. F. (2000). X-ray Structure Determinations of Li[CF3SO2N(CH2)3OCH3] and the Solid Electrolyte [Li⊂12-C-4][CF3SO2N(CH2)3OCH3]. Chemistry of Materials, 12(4), 1122–1126. https://doi.org/10.1021/cm990762x

[8] "LAMMPS Documentation." *LAMMPS Documentation - LAMMPS Documentation*, Sandia Corporation, 30 Mar. 2018, lammps.sandia.gov/doc/Manual.html.

[9] "VMD - Visual Molecular Dynamics." *Theoretical Biophysics Group*, University of Illinois at Urbana-Champaign, 27 Mar. 2018, www.ks.uiuc.edu/Research/vmd/.

[10] Meyer, W. H. (1998). Polymer Electrolytes for Lithium-Ion Batteries. Advanced Materials, 10(6), 439–448. https://doi.org/10.1002/(sici)1521-4095(199804)10:6<439::aid-adma439>3.0.co;2-i

[11] Cheng, X., Pan, J., Zhao, Y., Liao, M., & Peng, H. (2017). Gel Polymer Electrolytes for Electrochemical Energy Storage. Advanced Energy Materials, 8(7), 1702184. https://doi.org/10.1002/aenm.201702184

[12] Zhang, J., Sun, B., Huang, X., Chen, S., & Wang, G. (2014). Honeycomb-like porous gel polymer electrolyte membrane for lithium ion batteries with enhanced safety. Scientific Reports, 4(1). https://doi.org/10.1038/srep06007
[13] Picálek, J., & Kolafa, J. (2007). Molecular dynamics study of conductivity of ionic liquids: The Kohlrausch law. Journal of Molecular Liquids, 134(1–3), 29–33. https://doi.org/10.1016/j.molliq.2006.12.015
[14] Brown, J. R., Seo, Y., & Hall, L. M. (2018). Ion Correlation Effects in Salt-Doped Block Copolymers. Physical Review Letters, 120(12). https://doi.org/10.1103/physrevlett.120.127801